

# Cast iron zinc galvanizing improved by high temperature oxidation process

D. Jędrzejczyk\*, M. Hajduga

University of Bielsko-Biala, ul. Willowa 2, 43-309 Bielsko-Biala, Poland

\* Corresponding author: E-mail address: djedrzejczyk@ath.bielsko.pl

Received 27.09.2010; published in revised form 01.11.2010

## Manufacturing and processing

### ABSTRACT

**Purpose:** To evaluate influence of the high-temperature oxidation, as the preliminary stage previous to coating with zinc on the change of surface layer structure as well as subsurface layer of cast iron with flake, vermicular and nodular graphite.

**Design/methodology/approach:** The experiment was led in the temperature range: 850-1050°C in ambient air. Samples have been taken out from the furnace separately after: 2-12 hours. After scale layer removal the hot dip zinc coating in industrial conditions has carried out. Received effects were compared to these obtained during cast iron coating without preliminary thermal processing. To observation both optical and scanning microscope was applied. Sample's surface quality was described additionally by roughness measurements.

**Findings:** As the consequence of conducted high-temperature oxidation in subsurface layer of cast iron pores have been created, that in result of coating in liquid zinc were filled with new phase and in this way the new zone with different properties was obtained. Cast iron layer enriched in zinc is considerably thicker than layers got with application of other methods.

**Research limitations/implications:** It is suggested to verify the corrosion resistance of cast iron coated with zinc according to presented method and compare of got results with classic zinc coating effects.

**Practical implications:** The proposed method consisted on combining of hot dip zinc coating of cast iron with previous high temperature oxidation makes possible creation of sub-surface layer with composite character, composed of "after-graphite" voids filled with zinc and metallic matrix, without necessity of pressure processing.

**Originality/value:** New application of high temperature corrosion as the heat treatment improving effects obtained after cast iron zinc coating.

**Keywords:** High temperature oxidation; Hot dip zinc galvanizing; Cast iron

#### Reference to this paper should be given in the following way:

D. Jędrzejczyk, M. Hajduga, Cast iron zinc galvanizing improved by high temperature oxidation process, Journal of Achievements in Materials and Manufacturing Engineering 43/1 (2010) 418-423.

## 1. Introduction

In present work author decided to look at the high-temperature oxidation process from the point of view its influence on effects got during cast iron coating with Zn. The investigations of high-temperature corrosive resistance of cast iron have been led for tens years and they concern different aspects of this problem. The presented in literature results usually describe the

structure of cast iron scale layer or analyze the influence of different factors (the chemical composition of cast iron, shape of graphite, etc.) on oxidation mechanism [1-6]. The investigation of different grades of cast iron: with flake graphite, white, nodular and ductile showed that the oxidation kinetics and the scale layer morphology depend closely on size and distribution of flake graphite. With temperature increasing the process of oxidation accelerate, the scale layer porosity enlarges and the scale layer adhesiveness to metal core gets smaller [5].

Table 1.  
Chemical composition of cast iron applied in experiment

Graphite shape	Chemical composition, wg. %						
	C	Si	Mn	P	S	Mg	Ce
Flake	3.32	1.80	0.55	0.065	0.035	0	0
Nodular	3.63	2.55	0.10	0.025	0.007	0.045	0
Vemicular	3.65	2.58	0.08	0.023	0.008	0.025	0.015

Hot dip zinc galvanizing process is the most often used in industrial application to protect Fe-C alloys against corrosion influence of aggressive environment. Although the investigations are led from many years even now some problems exist in technology that can result in differentiation of coating thickness, increasing defects number and generally decrease the surface quality.

The corrosion resistance of zinc coating is determined by structure of created layer composed of few sub-layers. Published research describes mainly the mechanism of the zinc coating formatting at steel or crude surface of iron castings [7-10]. Meanwhile, a large majority of problems regard zinc coating of cast iron surface after machining. It follows from negative influence of graphite that can penetrate inside the coating and decrease its tightness (density). From the other side acids used in galvanizing technology can penetrate far inside along graphite interstitial surface and is very difficult to wash their away.

Introducing the new material into the pores' place (created as the result of high temperature oxidation in sub-surface layer of cast iron) may lead to: enlargement of thickness of subsurface cast iron layer enriched in zinc; obtaining composite surface layer with specific properties without necessity of expensive gear application.

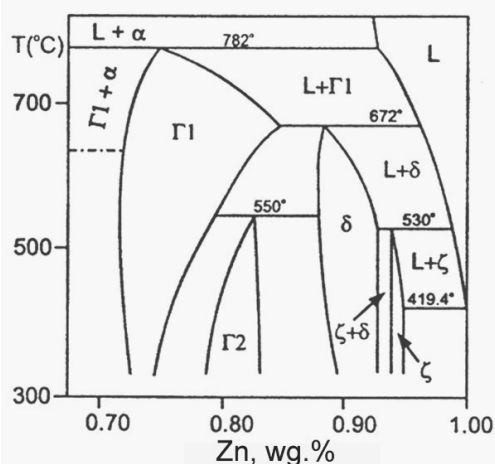


Fig. 1. Part of Fe-Zn equilibrium diagram from Zn side

For analysis of the zinc-coating structure created on iron alloys the basis is the Fe-Zn phase equilibrium diagram – Fig. 1 [11-13]. This diagram for several dozen years underwent many changes. About 80 years ago it was proved, that in Fe-Zn diagram occurs three phases, arising as a result of the peritectic reaction:  $\alpha$  -  $\text{Fe}_3\text{Zn}_{10}$ ,  $\delta$  -  $\text{FeZn}_7$ ,  $\zeta$  -  $\text{FeZn}_{13}$  and iron solid solution in zinc -  $\eta$ . Next research referred to different forms of  $\delta$  - phase existing

within different temperature range ( $\delta_1$ ,  $\delta$ ) and with different morphology ( $\delta_c$  – compacted,  $\delta_p$  – palisade). Also  $\gamma_2$  phase that is created as a result of reaction between  $\gamma_1$  and  $\delta$  phases was distinguished [10]. At present diagram showed at Fig. 1 is being regarded as a proper one. The sequence of phases creation in Fe-Zn diagram is presented at Fig. 2.

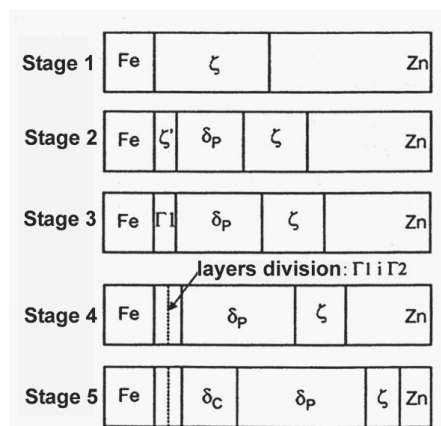


Fig. 2. The sequences of phases creation in Fe-Zn diagram

## 2. Method of investigation

During the investigations cast iron with flake, vemicular and nodular graphite melted in induction furnace of medium frequency was applied. Liquid metal was cast to sand mould with dimensions  $\phi 30 \times 300$  mm (cast iron with flake and vemicular graphite) and Y2 ingots (cast iron with nodular graphite). The chemical composition of applied cast iron is presented in Table 1.

From such cast ingots samples  $\phi = 11-19$  mm and length  $l = 110$  mm were turned. Then samples were put to sylite chamber furnace 600/25 to oxidize. The experiment was led in five different temperatures - 850, 900, 950, 1000 and 1050°C. Samples have been taken out from the furnace separately after: 2, 4, 6, 8, 10 and 12 hours. Before oxidation and after cooling dawn samples were exactly measured, weighed, and metallographic specimens were prepared to observe surface perpendicular to sample's axis.

The scale layer was removed in two stage procedure: mechanically by sandblasting as well as chemically by dipping in solution of oxalic acid. After scale layer removal the hot dip zinc coating in industrial conditions has carried out. Process consisted with the following action: degreasing – dirt and oil removal; pickling – rust, scale and carbon deposit removal; rinsing – hydrochloric acid removal; fluxing – increasing of zinc adhesion

to alloy; galvanizing in temperature 445-455°C; cooling – decreasing of sample temperature.

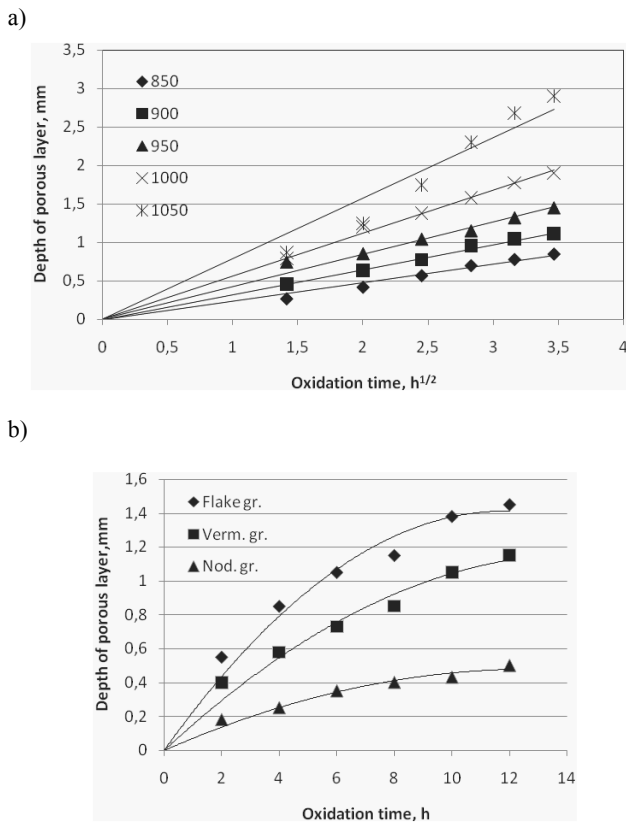


Fig. 3. Influence of different parameters on the porous layer depth: influence of temperature and time of oxidation – a (flake graphite); influence of graphite kind – b (950°C)

To optical observation microscope "NEOPHOT 2" as well as "Axiovert A -100" were applied, whereas further examination was made with application of scanning microscope "Jeol J7" and X-ray analyzer "JCXA – JEOL".

Sample's surface quality was described additionally by roughness measurements made after scale layer removal - „MAHR" profile measurement gauge with "Perthometer Concept" software.

### 3. Results of investigations and their analysis

The scale layer covering cast iron samples divide on two parts - first situated outside the initial surface of sample where porosity is directed parallel to the sample radius as well as internal layer where the direction of porosity is diverse. Additionally in subsurface layer of cast iron the area free from graphite which

thickness achieves 1.6 mm is observed. So generally the observed structure of cast iron can be divided on three layers. The conducted process of high-temperature oxidation leads to creation not only the scale layer and subsurface porous layer but also causes the change of metal matrix character from pearlitic to ferritic. Both measured parameters: the diameter of metal core as well as the samples mass enlarges more intensely in initial stage of oxidation. This is probably caused by growth of scale layer, which influence can be compared to the coat inhibiting the course of oxidation process. Additionally, the silicon content interaction can't be neglected; especially in cast iron where its value is much higher than in steel. Silicon favours the decrease the speed of oxidation, both during external, as well as internal corrosion.

The influence of oxidation parameters on thickness of porous layers obtained in grey cast iron with flake graphite and influence of graphite kind is presented at Fig. 3.

It follows from obtained dependence that porous layer thickness can be controlled by suitable selection of temperature and the time of oxidation as well as it depends on graphite shape existing in cast iron. Porous layer thickness decreases when graphite shape is changing from flake to vermicular and nodular.

Differentiation of the oxidation mechanism results from diverse graphite structure: flake and vermicular graphite precipitations are connected to each other, whereas nodular graphite precipitations are separated.

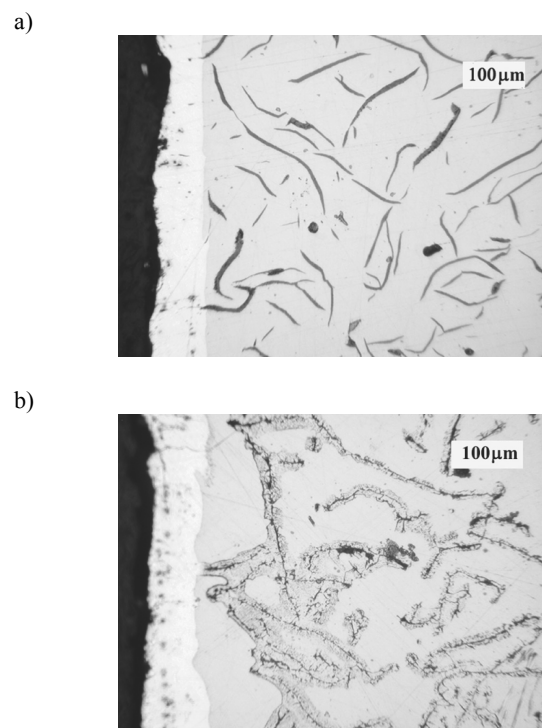


Fig. 4. Microstructure of cast iron with flake graphite after hot dip zinc galvanizing: a – zinc coating without oxidation; b – zinc coating with oxidation, 950°C, 8 hours, scale removed only mechanically

Table 2.

Results of X-ray point's analysis of measured elements concentrations – point's designation refers to Fig. 6b

Element concentration, wg %											
Point No.	O	Si	Fe	Cu	Zn	Point No.	O	Si	Fe	Cu	Zn
1	0.40	0.14	4.84	0.03	94.59	11	0.33	0.04	6.98	0.00	92.65
2	0.39	0.15	5.59	0.11	93.76	12	0.26	0.14	6.60	0.29	92.71
3	0.30	0.14	6.93	0.15	92.48	13	0.39	0.00	6.29	0.03	93.28
4	0.26	1.62	96.85	0.00	1.26	14	0.40	0.02	6.58	Mn=0.05	92.95
5	0.27	1.72	97.51	0.00	0.50	15	0.34	0.03	7.08	Mn=0.08	92.47
6	0.31	1.74	97.60	0.00	0.34	16	0.26	0.10	7.81	0.00	91.84
7	0.29	1.73	97.54	0.00	0.44	17	0.41	1.81	96.42	Mn=0.05	1.31
8	0.25	1.67	97.84	0.00	0.24	18	0.34	1.81	97.44	Mn=0.03	0.37
9	0.30	1.78	97.48	0.00	0.45	19	0.32	1.92	97.42	Mn=0.20	0.13
10	0.30	0.14	9.03	0.00	90.53	20	0.30	1.99	97.43	Mn=0.28	0.00

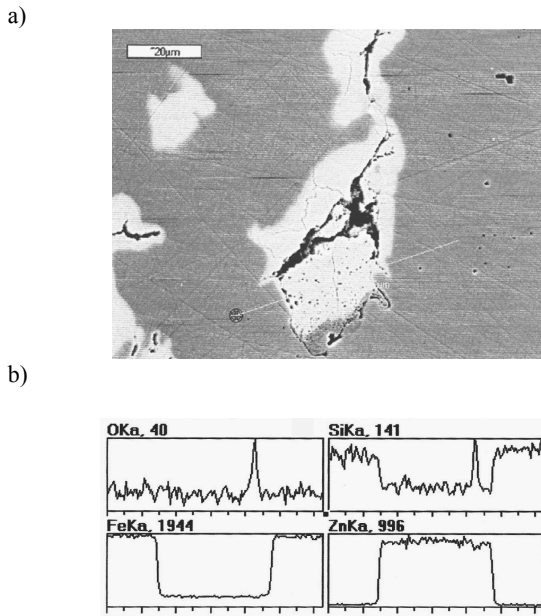


Fig. 5. Cast iron with vermicular graphite structure – a, together with linear distribution of analysed elements – b

Thickness of zinc layer that was created at the surface of cast iron samples is stable and reaches 70-100  $\mu\text{m}$ . The quality of obtained surface changes in dependence on parameters of high-temperature oxidation. The greatest surface smoothness -  $R_a < 6.3 \mu\text{m}$  was got for samples oxidized at parameters not higher than  $T \leq 1050^\circ\text{C}$  and  $t \leq 8\text{h}$ . For example, roughness measured at sample with flake graphite, that was oxidized before zinc coating ( $T=950^\circ\text{C}$ ,  $t=8\text{h}$ ) gained value  $R_a = 3.62 \mu\text{m}$ . It means decreasing in comparison to oxidized surface after sand blasting about  $3.26 \mu\text{m}$ . With reference to zinc coating of turned cast iron surface where initial roughness  $R_a = 1.13 - 2.34 \mu\text{m}$ , as the result of zinc coating, after putting the layer with thickness about  $100 \mu\text{m}$ , the surface with lower quality was obtained – the

roughness was in range  $3.5-4.1 \mu\text{m}$  (Fig. 4). Zinc layer observed at the cast iron surface not oxidized before has similar thickness to this one observed at the surface of oxidized samples, i.e. contained in range  $70-100 \mu\text{m}$ .

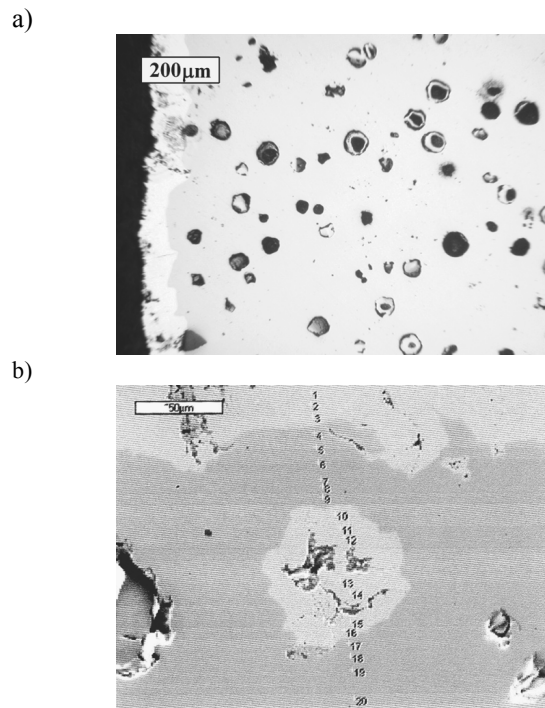


Fig. 6. Microstructure of cast iron with nodular graphite after oxidation and zinc coating with marked X-ray analysis points

Essential in this case is fact that graphite precipitation frequently penetrate in coated zinc layer and can in this way reduce it tightness (Fig. 4a). Such situation is not observed in case of oxidized cast iron. Cast iron, where the scale layer was

removed only mechanically – using sandblasting, does not reveal deep zinc penetration inside the “after-graphite” pores – it reach about 15  $\mu\text{m}$  (Fig. 4b).

Only when the chemical processing was used – dipping in solution of oxalic acid, the penetration depth considerable increase and achieves 120  $\mu\text{m}$  in cast iron with vermicular and flake graphite – Fig. 5.

In cast iron with nodular graphite, the depth of zinc penetration in considerable smaller, and resolve itself into filling the pores situated near the outside surface. Also in this case the filled with zinc precipitation can be observed even in distance 75  $\mu\text{m}$  from the surface.

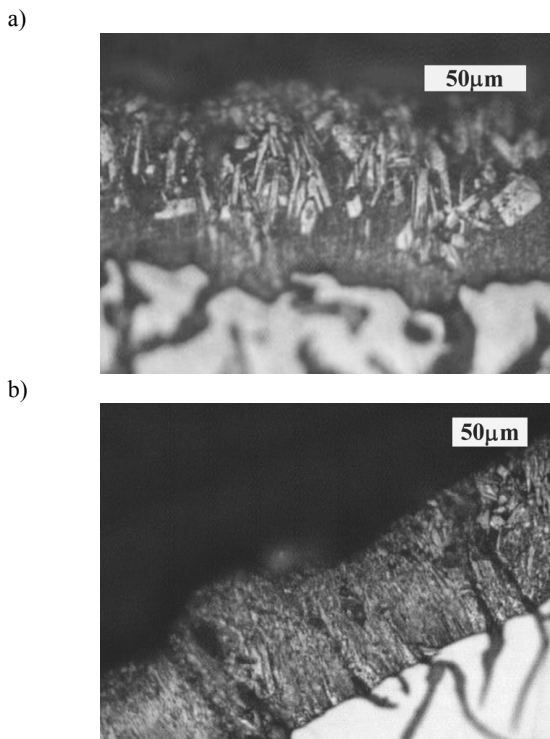


Fig. 7. Microstructure of alloyed Zn layer coated cast iron: a – cast iron after turning and oxidation; b – cast iron after turning

The X-ray analysis made in points presented at Fig. 6b – Table 2, shows that although the zinc content between outside zinc layer and the filled “after graphite” voids, changes gradually in the range (0.24-1.26%) and near the precipitation increase imperceptibly, we cannot found that the emptiness was filled by diffusion process. The infiltration character of “after-graphite” filling in cast iron with nodular graphite can be supported by graphite morphology - flake and vermicular graphite precipitations are connected to each other, whereas nodular graphite precipitations are separated. Occurrence of small precipitations numbers filled with zinc in nodular cast iron should be rather attributed to micro-cracks or assume that observed void

is the rounded end of vermicular graphite. The higher iron content in outside zinc sub-layer, that decrease with increasing of distance from cast iron surface confirms the growth model presented in literature and at Figs. 2 and 7. From the other side changes of zinc concentration between the coating and “after-graphite” filler, and also in direction from void to the core, prove intensification of zinc coating process as the result of “after-graphite” filling, that effect in widening of subsurface layer with increased zinc concentration. Without infiltration the enlarged zinc content was measured in distance 20  $\mu\text{m}$  from cast iron surface. Filling of the void with zinc resulted in described case in increasing of the zone with higher zinc concentration to 75  $\mu\text{m}$ .

## 4. Conclusions

1. The proposed method consisted on combining of hot dip zinc coating of cast iron with previous high temperature oxidation makes possible creation of sub-surface layer with composite character, composed of “after-graphite” voids filled with zinc and metallic matrix, without necessity of pressure processing.
2. To obtain such layer structure necessary is two-stage scale removal: mechanical – sandblasting and chemical. The use of only mechanical processing causes, that depth of zinc penetration gets lower to 15  $\mu\text{m}$  level.
3. Thickness of sub-surface layer where “after-graphite” pores are filled with zinc depends directly on kind of graphite. When the flake and vermicular/compacted graphite is observed depth of penetration reach 120  $\mu\text{m}$ , whereas in nodular cast iron it reach only 15  $\mu\text{m}$ , although sometimes single filled with zinc voids are observed at 75  $\mu\text{m}$  depth.
4. Roughness measured after zinc coating of cast iron being previously oxidized is sometimes even lower than roughness of zinc coating cast iron after turning. It follows first from negative influence of graphite precipitations uncovered during turning that can change locally the thickness and structure of coated layer and decrease in this way its tightness.
5. Considering the obtained results it looks very useful to verify the corrosion resistance of cast iron coated with zinc according to presented method and compare of got results with classic zinc coating effects.

## References

- [1] W. Kofstad, High Temperature Corrosion, Elsevier Applied Science, London, 1988.
- [2] K. Hauffe, Oxidation of Metals, Plenum Press, New York, 1965.
- [3] O. Kubaschewski, B.E. Hopkins, Oxidation of Metals and Alloys, Butterworths, London, 1967.
- [4] M. Hajduga, D. Jędrzejczyk, Z. Jurasz, Influence of Fe-samples diameter on the process of oxidation at high temperature, Proceedings of the 8<sup>th</sup> International

- Metallurgical Symposium METAL'99, Ostrava, 2009, 33-38.
- [5] H.D. Merchant, Oxidation behaviour of graphitic and white cast iron, Gordon and Breach, London, 1968.
- [6] C. Pehlan, Comparison between the oxidation of unalloyed and low alloyed cast iron with lamellar and spheroidal graphite, Georgi Publishing Company, 1975.
- [7] D. Kopyciński, E. Guzik, W. Wołczyński, Creation of the zinc layer at the surface of nodular cast iron industry fittings, *Materials Engineering* 4 (2006) 1081-1084 (in Polish).
- [8] D. Kopyciński, E. Guzik, W. Wołczyński, Coating Zn formation during hot dip galvanizing, *Materials Engineering* 4 (2008) 289-292.
- [9] J. Banaś, E. Guzik, D. Kopyciński, U. Lelek-Borkowaska, M. Starowicz, The effect of forming of zinc coating on their corrosion resistance, *Materials Engineering* 3-4 (2007) 750-756.
- [10] D. Kopyciński, E. Guzik, Zinc layer at the nodular cast iron surface. *Materials Engineering* 6 (2008) 780-783 (in Polish).
- [11] O. Kubaschewski, *Iron-Binary Phase Diagrams*, Berlin, Springer-Verlag, 1982.
- [12] P.B. Burton, P. Perrot, *Phase Diagram of Binary Iron Alloys*. American Society for Metals, Metal Park, OH, 1993, 459-466.
- [13] T.B. Masalski, *Binary Alloy Phase Diagrams*. ASM International, 1990.